Polymer 49 (2008) 5268–5275

Contents lists available at ScienceDirect

Polymer

journal homepage: www.elsevier.com/locate/polymer

Nanostructure and hydrogen bonding in interpolyelectrolyte complexes of poly(ε-caprolactone)-*block*-poly(2-vinyl pyridine) and poly(acrylic acid)

Nishar Hameed, Qipeng Guo*

Centre for Material and Fibre Innovation, Deakin University, Geelong, Victoria 3217, Australia

ARTICLE INFO

Article history:
Received 25 June 2008
Received in revised form 31 July 2008
Accepted 15 September 2008
Available online 1 October 2008

Keywords:
Block copolymers
Hydrogen bonding
Micelles

ABSTRACT

Nanostructured poly(ε-caprolactone)-*block*-poly(2-vinyl pyridine) (PCL-*b*-P2VP)/poly(acrylic acid) (PAA) interpolyelectrolyte complexes (IPECs) were prepared by casting from THF/ethanol solution. The morphological behaviour of this amphiphilic block copolymer/polyelectrolyte complexes with respect to the composition was investigated in a solvent mixture. The phase behaviour, specific interactions and morphology were investigated using differential scanning calorimetry (DSC), Fourier transform infrared (FTIR) spectroscopy, optical microscopy (OM), dynamic light scattering (DLS) and atomic force microscopy (AFM). Micelle formation occurred due to the aggregation of hydrogen bonded P2VP block and polyelectrolyte (PAA) from non-interacted PCL blocks. It was observed that the hydrodynamic diameter (D_h) of the micelles in solution decreased with increasing PAA content up to 40 wt%. After 50 wt% PAA content, D_h again increased. The micelle formation in PCL-*b*-P2VP/PAA IPECs was due to the strong intermolecular hydrogen bonding between PAA homopolymer units and P2VP blocks of the block copolymer. The penetration of PAA homopolymers into the shell of the PCL-*b*-P2VP block copolymer micelles resulted in the folding of the P2VP chains, which in turn reduced the hydrodynamic size of the micelles. After the saturation of the shell with PAA homopolymers, the size of the micelles increased due to the absorption of added PAA onto the surface of the micelles.

1. Introduction

A large amount of experimental and theoretical work has been done till date on the self-assembly and micellization of block copolymers [1–3]. It has been proven that amphiphiles can self-assemble into a large variety of microstructures. The micellization can provide information on the interactions between the components in the system and is thought to have important implications for biological studies [4–7]. Microphases formed by polymeric amphiphiles, compared to low molecular weight amphiphiles, are kinetically more stable, thus opening a variety of interesting applications such as nanocarriers for catalytic particles, molecules with electronic and photonic functions, and biological and medical species. The role of block copolymers in micelle formation is highly appreciated mainly from their unique solution and associative properties as a consequence of their molecular structure. For instance, amphiphilic diblock copolymers, such as poly(2-vinyl pyridine)-*block*-poly(ethylene oxide) (P2VP-*b*-PEO) [8], polystyrene-*block*-poly(ethylene oxide) (PS-*b*-PEO) [9], polystyrene-*block*-poly(acrylic acid) (PS-*b*-PAA) [10], polystyrene-*block*-poly(4-vinyl pyridine) (PS-*b*-P4VP) [11], and polystyrene-*block*-poly(2-cinnamoylethyl methacrylate) (PS-*b*-PCEMA) [12] can self-assemble into core–shell micelles with various morphologies in block-selective solvents.

The use of interpolymer interactions to trigger the complex formation and further study the aggregation has been implemented by many investigators [13–16]. In this, bond formation should only occur between the mutually interacting blocks which leads to the formation of microphase morphologies. Recent progress has demonstrated that these interactions can also induce polymer assembly in solutions [17,18]. An interpolymer interaction can significantly change the polymer solubility and conformation, which facilitates the formation of aggregates. The interactions can be electrostatic, hydrogen bonding, coordination bond or polar. Making use of such strong secondary interactions, one may greatly enhance the ability towards controlling novel and well-defined ordered nanostructures. Micelle formation in many block copolymer/homopolymer systems has also been studied extensively. Formation of spherical and cylindrical micelles, and hierarchical nanostructures was investigated in our previous work [19]. Gohy et al. [20] studied the micelle formation between PS-*b*-P4VP copolymers and PAA homopolymers in organic solvents, where the micelle core consisted of neat PS. Jiang and coworkers [21] investigated the micellization and stoichiometric complexation of PS-*b*-P4VP with formic acid (FA) in chloroform.

* Corresponding author. Tel.: +61 3 5227 2802; fax: +61 3 5227 1103.
E-mail address: qguo@deakin.edu.au (Q. Guo).

0032-3861/$ – see front matter © 2008 Elsevier Ltd. All rights reserved.
doi:10.1016/j.polymer.2008.09.032

However, though the addition of a polyelectrolyte into the block copolymer micelles has been investigated [22], a comprehensive analysis on the influence of hydrogen bonding on the micelle formation and morphology in such systems has not been explored well. Micelle formation in a stoichiometric mixture of poly(ε-caprolactone)-*block*-poly(2-vinyl pyridine)/poly(acrylic acid) (PCL-*b*-P2VP/PAA) taking place in THF/ethanol solvent mixture is investigated here. Such systems are usually known as inter-polyelectrolyte complexes (IPECs). Most studies including PAA have been focused on the assembly of single chains to form micelles under different conditions and the interactions of the resulting spherical micelles. The resulting core–shell micelles are usually considered thermodynamically frozen in solution. PAA is a polyelectrolyte and is thus strongly sensitive to the surrounding conditions. Thus most of the investigations are based on the response of the PAA blocks or homopolymers to the pH of the solution, which may affect the structure of the micelles [10,22]. Here, we investigate the effect of stepwise addition of the polyelectrolyte solution into an amphiphilic diblock copolymer which already exists as aggregate micelles in a solution mixture. The micelles formed here are termed as complex coacervate micelles, or precisely complex coacervate shell micelles since the shell of the micelles is composed of oppositely charged PAA and P2VP. A similar system where the core of the micelles was composed of oppositely charged blocks was studied by Voets et al. [23]. In their system, the micelles are termed as complex coacervate core micelles because the core consists of the oppositely charged polyelectrolyte blocks PAA and poly(2-methylvinylpyridinium iodide) (P2MVP), whereas the corona consists of neutral poly(acrylamide) (PAAm) blocks. The micelle formation and the hydrodynamic diameter (D_h) of the micelles were confirmed by dynamic light scattering (DLS), the microphase morphology was examined using atomic force microscope (AFM) and the semi-crystalline morphology of the IPECs was examined using polarizing optical microscope (POM). The effect of hydrogen bonding interactions on the morphological changes was investigated using Fourier transform infrared (FTIR) spectroscopy and the phase behaviour of the IPECs was analyzed with differential scanning calorimetry (DSC).

2. Experimental section

2.1. Materials and methods

The polymers used in the present study were poly(acrylic acid) (PAA) and poly(ε-caprolactone)-*block*-poly(2-vinyl pyridine) (PCL-*b*-P2VP). PAA with an average $M_w = 1800$ was obtained from Aldrich Chemical Company, Inc. The PCL-*b*-P2VP copolymer was from Polymer Source, Inc., with M_n (P2VP) = 20,900, M_n (PCL) = 26,100 and $M_w/M_n = 1.11$. The block copolymer PCL-*b*-P2VP was first dissolved in THF to make a 0.5% (w/v) of polymer solution followed by the slow addition of ethanol. Ethanol solution containing 0.5% (w/v) of PAA homopolymer was prepared separately. Interpolyelectrolyte complexes were prepared by slowly adding PAA solution into PCL-*b*-P2VP solution. The resultant solution was kept for complete precipitation. The solvent was allowed to evaporate slowly at room temperature.

2.2. Fourier transform infrared (FTIR) spectroscopy

The KBr disk method was adopted to determine the FTIR characteristics of the IPECs. The FTIR spectra of all the samples were measured on a Bruker Vetex-70 FTIR spectrometer. The sample solution was cast onto KBr disk, solvent was allowed to evaporate slowly at room temperature. The disks were dried under vacuum in an oven before taking the measurements. The spectra were recorded at the average of 32 scans in the standard wavenumber range of 400–4000 cm^{-1} at a resolution of 4 cm^{-1}.

2.3. Differential scanning calorimetry (DSC)

The thermal behaviour of the IPECs was analyzed by a Perkin–Elmer Diamond DSC. The measurement was performed using 5–10 mg of the sample under an atmosphere of nitrogen gas. The samples were first heated to 100 °C and held at that temperature for 3 min to remove the thermal history. Then the samples were cooled to −50 °C at a rate of 20 °C/min, held for 5 min and again heated from −50 to 200 °C at 20 °C/min. The glass transition temperature (T_g) was taken as the midpoint of transition and melting temperature (T_m) was taken as the maximum of the endothermic peak in the DSC thermograms.

2.4. Polarizing optical microscopy (POM)

The semi-crystalline morphology of PCL-*b*-P2VP/PAA IPECs was analyzed using a Nikon eclipse-80*i* optical microscope under polarized light. The solutions of the IPECs were spread as thin films on the glass slides and dried in vacuum oven.

2.5. Dynamic light scattering (DLS)

In DLS [24], an autocorrelation function plots the average overall change in intensity with time, for a given time interval which is given by,

$$G(\tau) = \int I(t)I(t+\tau)\mathrm{d}t \tag{1}$$

where t is the delay time. In DLS, all the information regarding the motion or diffusion of particles in the solution is embodied within the measured correlation curve, which can be fit to a single exponential form i.e.,

$$\int I(t)I(t+\tau)\mathrm{d}t = B + A\exp\left[-2q^2D\tau\right] \tag{2}$$

where B is the baseline, A is the amplitude, q is the scattering vector ($q = 4\pi r \sin[\theta/2]$, r is the refractive index of the solvent) and D is the diffusion coefficient.

The diffusion coefficient is calculated by fitting the correlation curve to an exponential function, where D is proportional to the exponential decay time. The hydrodynamic diameter (D_h) can be calculated using the particle diffusion coefficient and Stokes–Einstein equation given below, where k is the Boltzmann constant, T is the temperature, η is the refractive index, and h is the dispersant viscosity.

$$D_h = kT/3\pi\eta D \tag{3}$$

DLS measurements were performed with a spectrometer (Zetasizer Nano ZS) equipped with He–Ne laser with a wavelength of 633 nm digital correlator. All measurements were carried out at 25 °C, with a detection angle of 173°. Solutions of 0.5% (w/v) complex aggregates in ethanol/THF were used. The scattering intensity autocorrelation functions were analyzed using the methods of CONTIN and Cumulant which are based on an inverse-Laplace transformation of the data and give access to a size distribution histogram for the analyzed solutions.

2.6. Atomic force microscopy (AFM)

The phase morphology of the IPECs was examined using an AFM (DME type DS 45-40, Denmark) in the tapping mode at room temperature. The thin films of the samples were prepared on glass slides. The samples were annealed for 72 h under vacuum. The height and phase images were recorded simultaneously while operating the instrument in the tapping mode.

3. Results and discussion

3.1. Hydrogen bonding interactions

The FTIR spectra of PCL-*b*-P2VP/PAA IPECs in the region 1800–4000 cm^{-1} are given in Fig. 1. It can be noticed that pure PAA exhibits some characteristic bands in this region. The broad band in the region 2800–3300 cm^{-1} can be attributed to the O–H stretching and the band at 2647 cm^{-1} corresponds to the 'satellite' band. According to Lee et al. [25], these satellite bands arise due to some overtones and combinations owing to different stretching modes. The spectra of the IPECs show two new bands at 2530 and 1930 cm^{-1}. These bands arise due to the intermolecular interaction between the carboxylic groups in PAA and pyridine groups in P2VP.

The FTIR spectra of PCL-*b*-P2VP/PAA IPECs in the region 1650–1780 cm^{-1} are given in Fig. 2. This region is quite complicated since both PAA and PCL show characteristic absorption bands due to the presence of carbonyl groups. The two carbonyl bands of pure PCL-*b*-P2VP, one relatively sharp at 1725 cm^{-1} and the other seen as a shoulder at 1736 cm^{-1} can be attributed to crystalline and amorphous conformations of PCL, respectively. Pure PAA exhibits a broad band at 1710 cm^{-1} which can be attributed to the overlapping of two carbonyl stretching bands comprising of free as well as self-associated carboxylic groups in PAA. This band moves towards higher wavenumbers upon complex formation and a sharp band appears at 1730 cm^{-1} in the spectra of PCL-*b*-P2VP/PAA IPECs as shown in Fig. 2. This behaviour is schematically represented in Fig. 3. However, since both PCL and PAA exhibit bands in this region, the observed band at 1730 cm^{-1} region could be resulted from the overlapping of contributions from these two bands. The interaction between PAA and P2VP blocks of PCL-*b*-P2VP block copolymer can

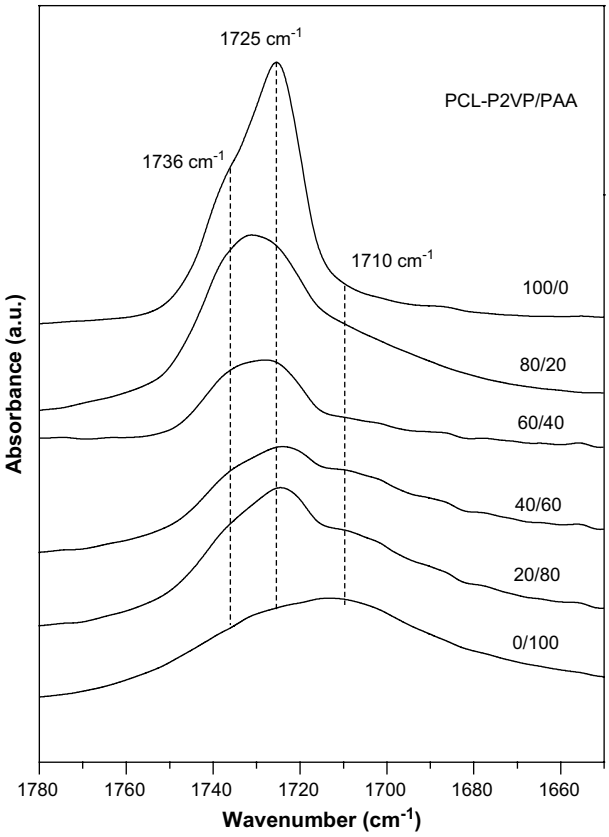

Fig. 2. Infrared spectra in the carbonyl stretching region of PCL-*b*-P2VP/PAA IPECs at room temperature.

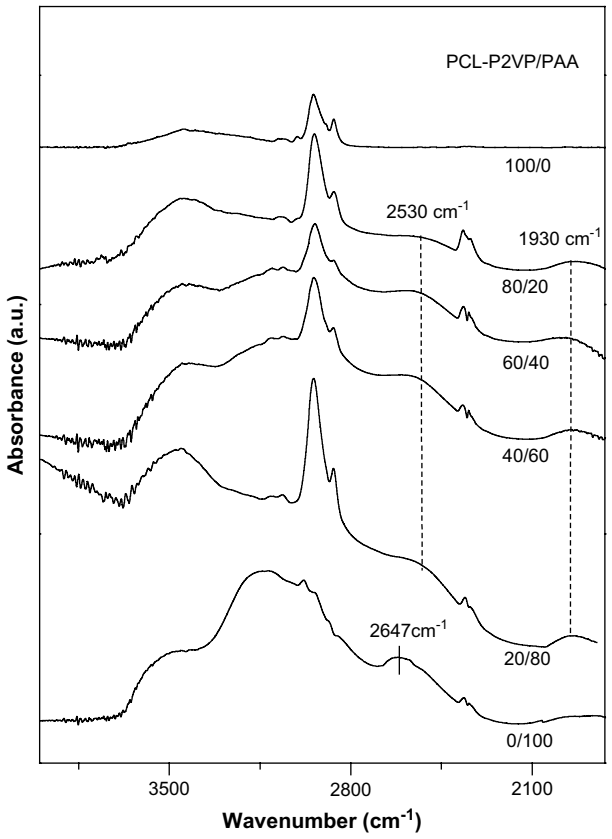

Fig. 1. Infrared spectra in the region of 1800–4000 cm^{-1} of PCL-*b*-P2VP/PAA IPECs at room temperature.

be examined by analysing the 1550–1610 cm^{-1} region in the IR spectra of IPECs which are given in Fig. 4. Pure P2VP exhibits two peaks at 1568 and 1591 cm^{-1}, respectively which are the ring modes of pyridine group. The band at 1591 cm^{-1} becomes broad and shifts towards higher wavenumbers as the PAA content increases in the IPEC, which is due to the increase in stiffness of the pyridine ring as a result of hydrogen bonding [26]. The hydrogen bonded pyridine band is observed at 1596 cm^{-1} in the complex. It is possible to calculate the quantitative fraction of hydrogen bonded pyridine groups in the IPECs. The fraction of hydrogen bonded pyridine groups can be calculated using the equation,

$$f_b = \frac{A_b/a}{A_b/a + A_f} \tag{4}$$

where A_f and A_b are the peak areas of the free and hydrogen bonded pyridine groups. The conversion constant a is the specific

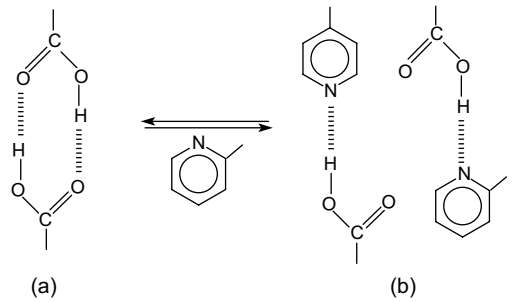

Fig. 3. Formation of free carbonyl groups due to the intermolecular hydrogen bonding in PCL-*b*-P2VP/PAA IPECs: (a) self-associated PAA and (b) inter-associated PAA and P2VP with the liberated carbonyl groups.

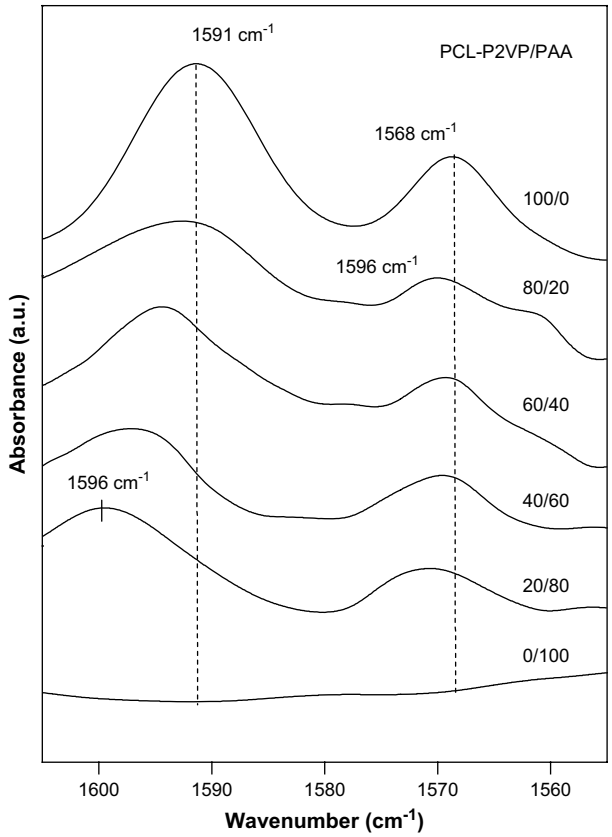

Fig. 4. Infrared spectra in the region of 1560–1610 cm^{-1} of PCL-*b*-P2VP/PAA IPECs at room temperature.

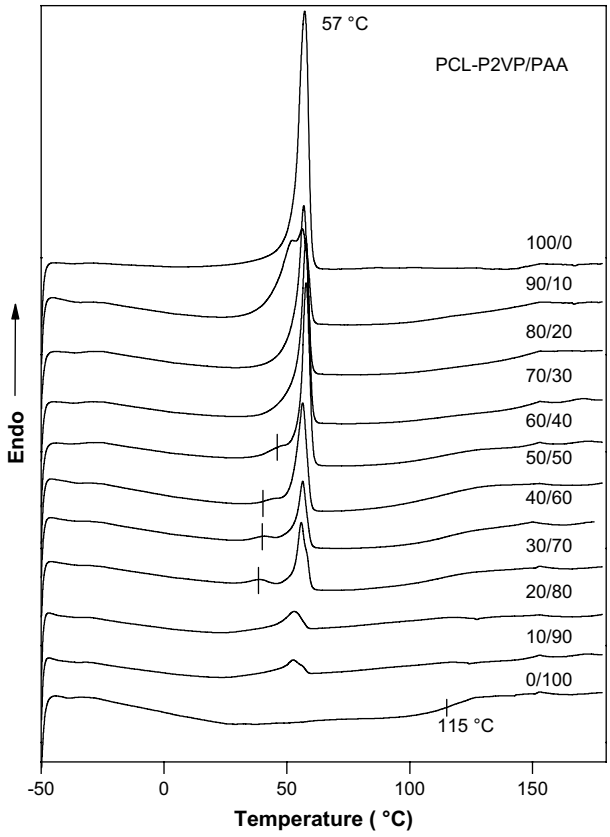

Fig. 5. DSC curves of the second scan of PCL-*b*-P2VP/PAA IPECs.

absorption ratio of the above two bands. The value of $a = 1$, as has been reported for other systems where vinyl pyridines (VPs) are mixed with hydrogen donor polymer [27]. The results from curve fitting at room temperature are summarized in Table 1. From the table it is clear that the fraction of hydrogen bonded pyridine groups increases with increasing PAA content.

3.2. Phase behaviour

The thermal behaviour of PCL-*b*-P2VP/PAA IPECs was examined using DSC. The DSC curves of the second scan (heating) of IPECs at various compositions are shown in Fig. 5. The IPECs contain the block copolymer PCL-*b*-P2VP with two immiscible blocks, which is supposed to exhibit two separate T_gs corresponding to PCL block and P2VP block, respectively. However, the T_g of PCL blocks is not detectable from the DSC curves under the current experimental conditions. From the DSC analysis, PAA shows a T_g at 115 °C, and in the block copolymer, P2VP exhibits T_g approximately at 102 °C. The T_g values of the IPECs are plotted against the composition as is shown in Fig. 6. The IPECs exhibit a single T_g corresponding to the homogeneous PAA/P2VP phase. This can be attributed to the high degree of mixing between the two polymers due to strong intermolecular hydrogen bonding.

The melting points of immiscible PCL phase can be detected from DSC curves. Melting point depression, which is an important characteristic of polymer mixtures where intermolecular interactions exist, cannot be observed in this complex. The pure block copolymer exhibits a peak at 57 °C which is the melting point of crystalline PCL blocks [27]. However, in PCL-*b*-P2VP/PAA IPECs, the melting point remains unchanged with increase in PAA content. From Fig. 5, it can be observed that PCL melting peak can be observed even at 90 wt% PAA IPECs. Meanwhile, the complex with 20–50 and 90 wt% PAA shows crystallization exotherms during heating. This indicates that PCL becomes difficult to crystallize, suggesting a gradually decreased crystallization rate. It can be concluded that PCL phase was not involved in any kind of intermolecular attraction in the IPECs.

The semi-crystalline morphology of the PCL-*b*-P2VP/PAA IPECs was examined using the optical microscope. The ethanol/THF cast complex films were analyzed at different magnifications. The polarizing optical microscopic (POM) images are given in Fig. 7. From the figure it is clear that the IPECs contain PCL crystalline spherulites. As the concentration of PAA increases in the IPECs, the

Table 1
Curve fitting results of PAA/P2VP interactions in PCL-*b*-P2VP/PAA IPECs at room temperature

PCL-*b*-P2VP/PAA	Free pyridine group			Bonded pyridine group			f_b (%)
	ν (cm^{-1})	$W_{1/2}$ (cm^{-1})	A_f (%)	ν (cm^{-1})	$W_{1/2}$ (cm^{-1})	A_b (%)	
20/80	1591	16.3	19.6	1596	12.6	80.4	80.4
40/60	1591	129	26.1	1596	14.6	73.9	73.9
60/40	1591	18.8	47.9	1596	13.9	52.1	52.1
80/20	1591	15.2	78.7	1596	16.2	21.3	21.3

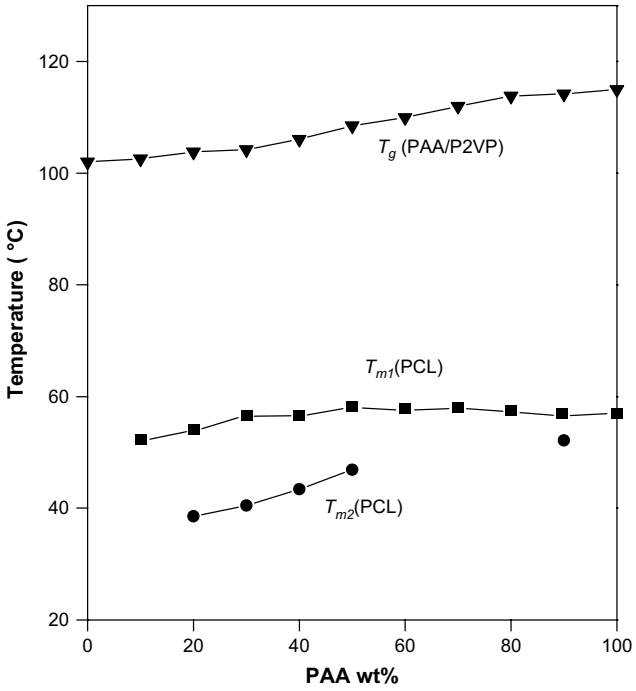

Fig. 6. Glass transition temperature vs composition during the second scan of PCL-*b*-P2VP/PAA IPECs.

spherulites become smaller, however, can be observed even at very high PAA concentrations.

3.3. *Micelle formation*

The PCL-*b*-P2VP/PAA IPECs are prepared by slowly adding PAA in ethanol solution into PCL-*b*-P2VP in THF solution, because ethanol is a common solvent for both PAA and P2VP block of the block copolymer, but a precipitant for the PCL block. Core–shell micelles with PCL blocks as the core and hydrogen bonded P2VP/PAA phase as the shell are formed when both solutions are mixed together. These micelles are called complex coacervate shell micelles since the shell of the micelles is composed of oppositely charged PAA and P2VP.

When PAA in ethanol solution is dropped into the PCL-*b*-P2VP in THF/ethanol solution, four different components exist in the solution mixture, such as PCL-*b*-P2VP, PAA units, ethanol and THF. Hydrogen bonding takes place not only between pyridine units and acrylic acid units but may also exist between pyridine units and ethanol, pyridine units and THF, acrylic acid units and ethanol, and carbonyl units and THF. Thus, the final morphology of the complex is the result of balance of all these factors. Of the four components, the PAA block is the strongest Lewis acid and P4VP is the strongest Lewis base; thus, hydrogen bonging between PAA units and P2VP blocks should be the most predominant.

The micelle formation of PCL-*b*-P2VP/PAA IPECs in solution was analyzed using DLS. Fig. 8 shows the plots of the hydrodynamic diameter (D_h) distribution of the core–shell micelles vs intensity at 20 °C at different compositions. For each complex solution, the size distribution consists of a single peak with a narrow size distribution. Moreover, it can be noted that the peak of the IPECs shifts with the increasing PAA content. This is obviously due to the swelling of the block copolymer by PAA homopolymer. Micelles with different size distributions are formed in the solution at different compositions. The D_h–composition and polydispersity index (PDI)–composition plots are given in Fig. 9. Polydispersity in the area of light scattering is used to describe the width of the particle size distribution. Here, the term polydispersity is derived from the polydispersity index, a parameter calculated from a Cumulants analysis of the DLS measured intensity autocorrelation function.

It can be observed that the D_h of the micelles decreases initially with increasing concentration of the PAA content. There is a gradual decrease in D_h of the micelles till 40 wt% of PCL-*b*-P2VP/PAA IPECs and increases thereafter. The PCL-*b*-P2VP diblock copolymer exists in solution as spherical core–shell micelles with PCL chains as the

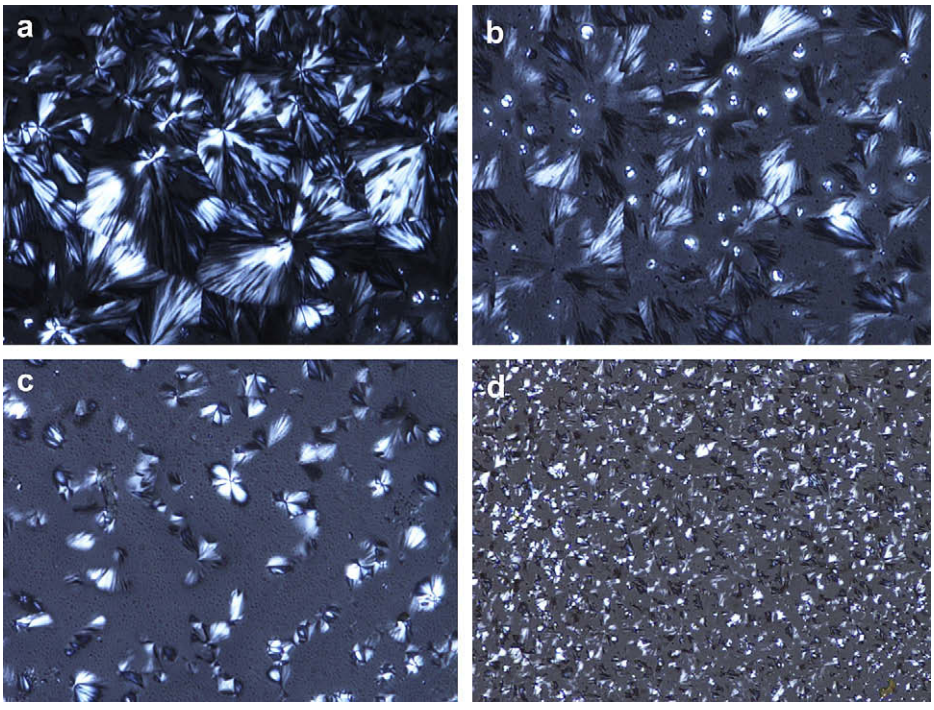

Fig. 7. POM images of (a) 100/0, (b) 70/30, (c) 40/60, and (d) 20/80 PCL-*b*-P2VP/PAA IPECs.

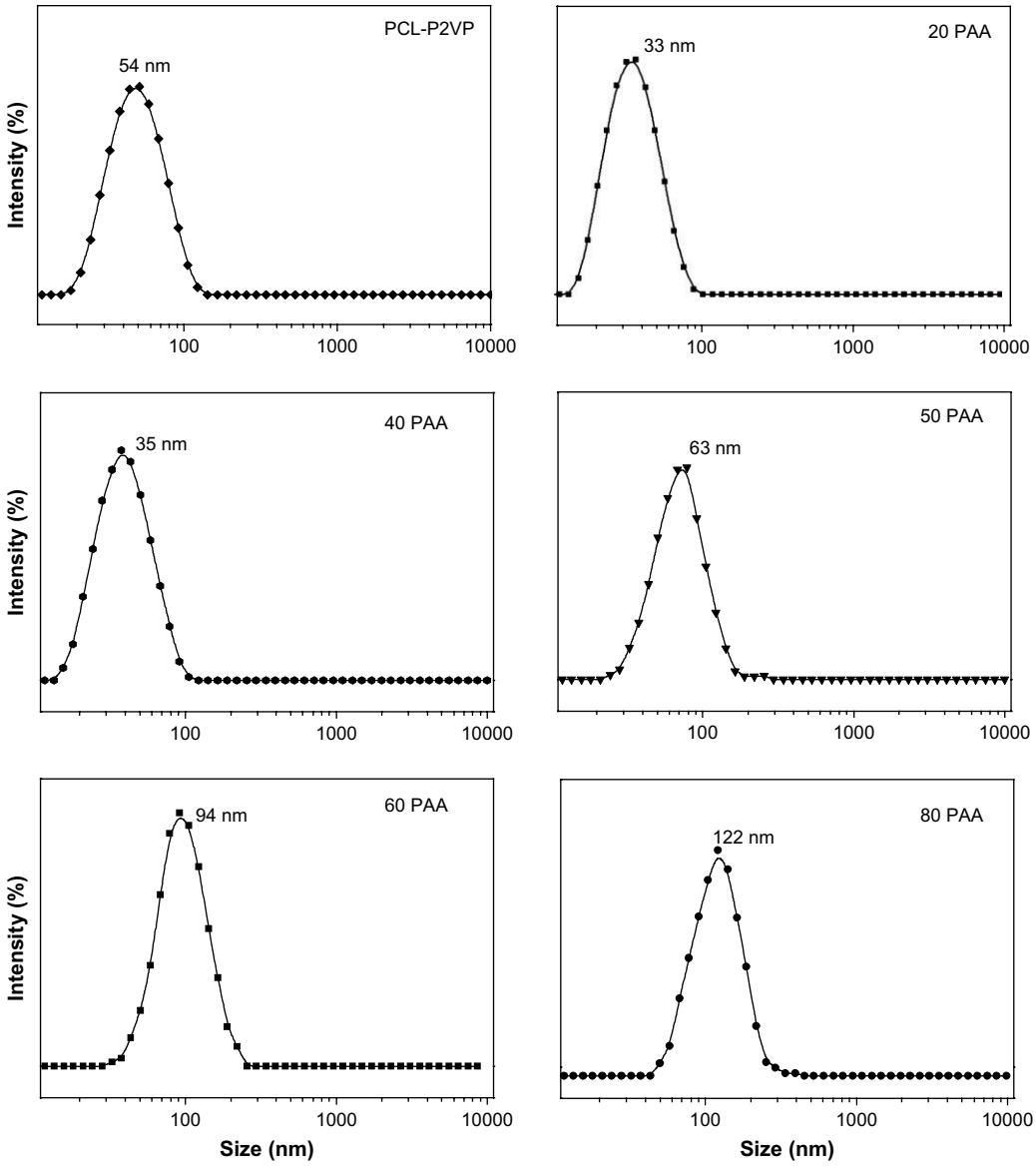

Fig. 8. Hydrodynamic diameter (D_h) distribution of 100/0, 80/20, 60/40, 50/50, 40/60 and 20/80 PCL-*b*-P2VP/PAA IPECs in 0.5% (w/v) tetrahydrofuran (THF)/ethanol solution mixture.

core and P2VP chains as the shell. When PAA solution is added to the PCL-*b*-P2VP solution, PAA units are absorbed into the shell of the core–shell micelles due to the hydrogen bonding between PAA and shell forming P2VP blocks. The decrease in diameter can be attributed to the strong hydrogen bonding induced absorption of PAA units to the PCL-*b*-P2VP micelles. This reduction in diameter continues till saturated amount of PAA is absorbed by P2VP blocks. When an excess amount of PAA is further added (above 40 wt% PAA), the PAA units are added onto the surface of the shell which causes the increase in diameter of the micelles. In hydrogen bonding interactions, unlike electrostatic interactions or hydrophobic interactions, the absorbed PAA units can be penetrated into the shell of PCL-*b*-P2VP micelles. Moreover, upon the addition of PAA in ethanol, the P2VP chains in the shell can stretch into the solution since they are soluble in ethanol. The hydrogen bonding between PAA and P2VP changes the conformation of the P2VP chains from stretched to folded that results in the reduction in size. In DLS, the average size is derived as the intensity weighed average hydrodynamic size of the collection of particles being measured, which is simply influenced by the hydration or solvation effects. In microscopic measurements, on the other hand, it is the number weighed average size of the dehydrated sample. Hence the average diameter of the particles calculated from DLS is always slightly higher than the AFM or TEM measurements.

The morphology of the solid IPECs was examined with AFM. The phase images of PCL-*b*-P2VP/PAA IPECs at various compositions are given in Fig. 10. Spherical micelles are observed in all the complex compositions. The phenomena of reduction in diameter of the micelles, however, cannot be analyzed precisely since the average diameter of the spherical micelles in the solid sample is almost the same at lower PAA concentrations. However, it can be observed from Fig. 10 that there is no noticeable increase in the micelle diameter till 40 or 50 wt% PAA IPECs. The micelles at 80 or 90 wt% PAA IPECs appear to be larger compared to the lower concentrations. Therefore, the result is consistent with the DLS experiments.

The formation mechanism of different microphases in PCL-*b*-P2VP/PAA IPECs at different compositions is illustrated in Fig. 11. Fig. 11a shows a schematic representation of PCL-*b*-P2VP block copolymer micelles in THF/ethanol solvent mixture. Here, the PCL blocks, which are insoluble in ethanol, form the core of the micelle

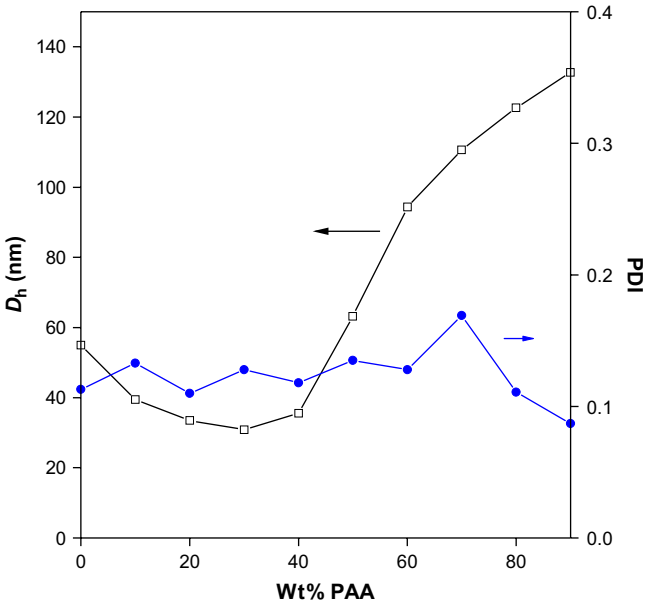

Fig. 9. Hydrodynamic diameter (D_h) vs composition and polydispersity index (PDI) vs composition of PCL-*b*-P2VP/PAA IPECs in 0.5% (w/v) tetrahydrofuran (THF)/ethanol solution mixture.

while the P2VP blocks which are soluble in both ethanol and THF form the shell. Therefore, P2VP chains are quite relaxed and can stretch freely into the solution. The size of the core–shell micelles is about 50 nm in solution as determined by DLS. In the IPECs containing 10 wt% of PAA, the size of the micelles changes (Fig. 11b) as a result of addition of PAA homopolymers. The added PAA forms strong hydrogen bonds with the P2VP shell and which changes the

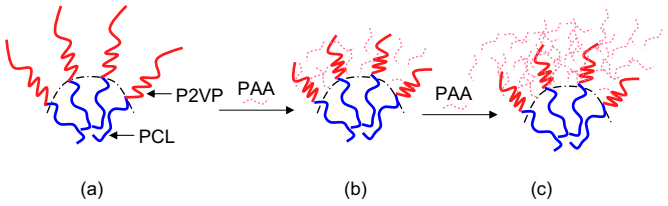

Fig. 11. Schematic representation of complex coacervate shell micelles formation and absorption of PAA in PCL-*b*-P2VP/PAA IPECs: (a) PCL-*b*-P2VP block copolymer micelles, (b) 90/10, and (c) 50/50 PCL-*b*-P2VP/PAA complex micelles.

shell conformation into folded structure. The absorption of PAA homopolymers into the shell causes the reduction in the hydrodynamic size of the micelles. This reduction in size continues till 40 wt% PAA IPECs. The size of the micelle aggregates increases (Fig. 11c) after 50 wt% PAA IPECs; this may be due to the saturated amount of PAA in the shell. The added PAA homopolymers are absorbed onto the surface of the micelles which results in the increased hydrodynamic size of the micelles. However, the reduction in hydrodynamic size can be identified only in DLS studies. The AFM images give no information about the reduction in size of the micelles at lower PAA content. This is because the stretching and folding of the P2VP chains can happen only in solutions. Since the samples were thermally annealed, AFM provided only the morphology of the dry solid surface.

4. Conclusions

The micellization in PCL-*b*-P2VP/PAA interpolyelectrolyte complexes was observed as a function of composition. Core–shell micelles were formed by the mutual mixing of polyelectrolyte PAA in ethanol and PCL-*b*-P2VP in THF/ethanol solutions. This complex

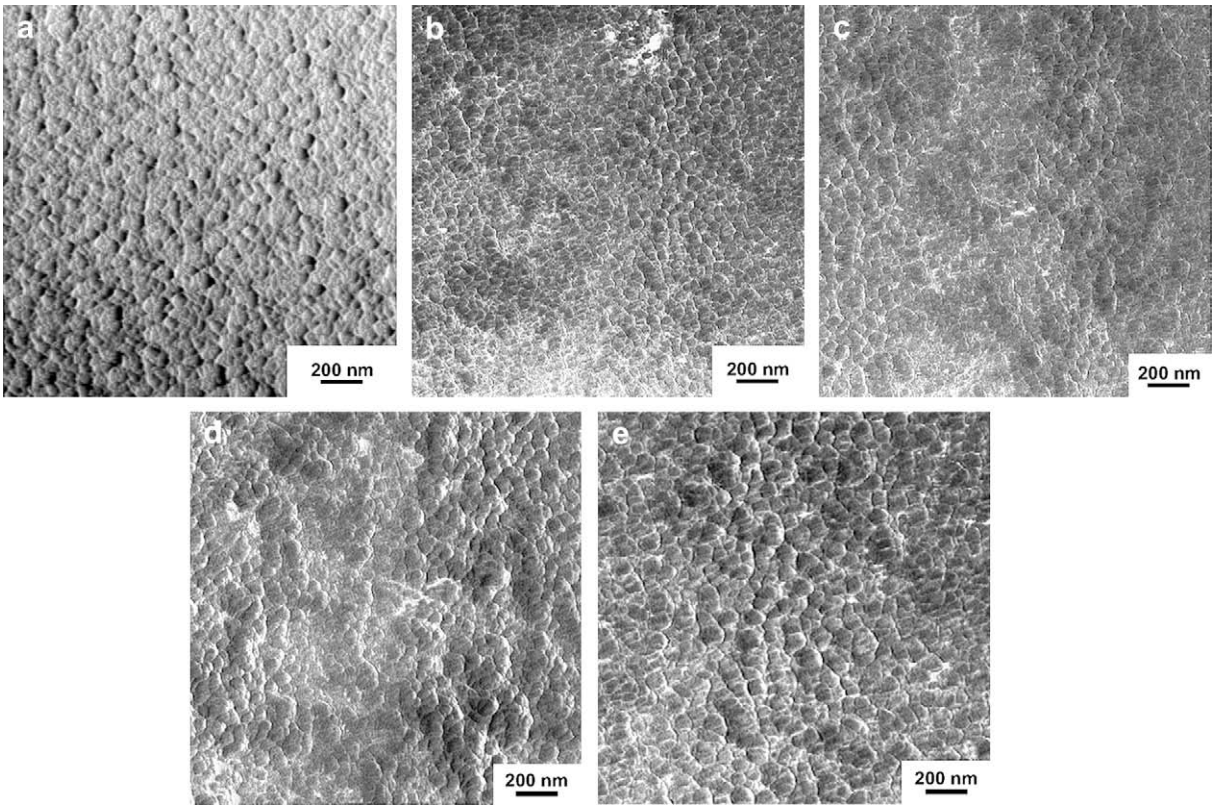

Fig. 10. AFM images of (a) 100/0, (b) 90/10, (c) 70/30, (d) 50/50, and (e) 20/80 PCL-*b*-P2VP/PAA IPECs.

coacervate shell micelles were composed of hydrogen bonded PAA/P2VP shell and with non-interacting PCL blocks as the core. The hydrogen bonding interaction in the IPECs was revealed by FTIR results. The PCL blocks showed crystallinity even at very high PAA contents. The absorption of PAA homopolymer units into the shell of PCL-*b*-P2VP micelles was confirmed by the decrease in the hydrodynamic radius of the micelles with increase in PAA concentration up to 40 wt%. The reduction in size of the micelles was attributed to the penetration of PAA homopolymer units into the P2VP shell, since P2VP and PAA form very strong intermolecular hydrogen bonding. The size of the micelles again increased after 50 wt% PAA IPECs, which is attributable to the saturation of PAA groups in the shell of the micelles.

Acknowledgments

This work was financially supported by the Australian Research Council under the Discovery Project Scheme and by Deakin University through a CRGS grant. One of us (N.H.) would like to express his gratitude for a DUIRS scholarship from Deakin University.

References

[1] Tuzar Z, Kratochvil P. Micelles of block and graft copolymers in solution, Surface and colloid science. New York: Plenum Press; 1993.
[2] Hamley IW. Block copolymers. Oxford: Oxford University Press; 1999.
[3] Alexandridis P, Lindman B. Amphiphilic block copolymers: self assembly and applications. Amsterdam: Elsevier; 2000.
[4] Zhu H, Liu Q, Chen Y. Langmuir 2007;23:790.
[5] Choi H, Brooks E, Montemagno CD. Nanotechnology 2005;16:143.
[6] Uchegbu IF. Expert Opin Drug Delivery 2006;3:629.
[7] Allena C, Hana J, Yua Y, Maysinger D, Eisenberg A. J Controlled Release 2000;63:275.
[8] Martin TJ, Prochazka K, Munk P, Webber SE. Macromolecules 1996;29:6071.
[9] (a) Yu K, Eisenberg A. Macromolecules 1996;29:6359;
(b) Zhao C, Winnik MA, Riess G, Croucher MD. Macromolecules 1990;6:514;
(c) Xu R, Winnik MA, Hallett FR, Riess G, Croucher MD. Macromolecules 1991;24:87.
[10] (a) Zhang L, Eisenberg A. Science 1995;268:1728;
(b) Zhang L, Eisenberg A. J Am Chem Soc 1996;118:3168;
(c) Zhang W, Shi L, An Y, Gao L, Wu K, Ma R. Macromolecules 2004;37:2551.
[11] (a) Khougaz K, Gao Z, Eisenberg A. Macromolecules 1994;27:6341;
(b) Shen H, Zhang L, Eisenberg A. J Am Chem Soc 1999;121:2728.
[12] (a) Underhill RS, Ding J, Birss VI, Liu G. Macromolecules 1997;30:8298;
(b) Ding J, Liu G. Macromolecules 1999;32:8413;
(c) Tao J, Stewart S, Liu G, Yang M. Macromolecules 1997;30:2738.
[13] Antonietti M, Conrad J, Thünemann A. Trends Polym Sci 1997;5:262.
[14] Mogi Y, Nomura M, Kotsuji H, Ohnishi K, Matsushita Y, Noda I. Macromolecules 1994;27:6755.
[15] Gido SP, Schwark DW, Thomas EL, Goncalves MC. Macromolecules 1993;26:2636.
[16] (a) Zhong Z, Guo Q. J Polym Sci Part B Polym Phys 1999;37:2726;
(b) Huang J, Li X, Guo Q. Eur Polym J 1997;33:659;
(c) Zhong Z, Guo Q. J Polym Sci Part A Polym Chem 1998;36:401;
(d) Guo Q, Harratsa C, Groeninckx G, Koch MHJ. Polymer 2001;42:4127;
(e) Guo Q, Harratsa C, Groeninckx G, Reynaers H, Koch MHJ. Polymer 2001;42:6031.
[17] (a) Kabanov AV, Bronich TK, Kabanov VA, Yu K, Eisenberg A. J Am Chem Soc 1998;120:9941;
(b) Zhou S, Chu B. Adv Mater 2000;12:54;
(c) Gohy JF, Varshney SK, Jerome R. Macromolecules 2001;34:3361;
(d) Schrage S, Sigel R, Schlaad H. Macromolecules 2003;36:1417;
(e) Weaver JVM, Armes SP, Liu S. Macromolecules 2003;36:9994.
[18] (a) Zhang GZ, Liu S, Zhao H, Jiang M. Mater Sci Eng C 1999;10:155;
(b) Liu S, Zhu H, Zhao H, Jiang M, Wu C. Langmuir 2000;16:3712;
(c) Liu X, Jiang M, Yang S, Chen M, Chen D, Yang C, et al. Angew Chem Int Ed 2002;41:2950;
(d) Chen D, Jiang M. Acc Chem Res 2005;38:494;
(e) Ilhan F, Galow TH, Gray M, Clavier G, Rotello VM. J Am Chem Soc 2000;122:5895;
(f) Percec V, Dulcey AE, Balagurusamy VSK, Miura Y, Smidrkal J, Peterca M, et al. Nature 2004;430:764;
(g) Hu J, Liu G. Macromolecules 2005;38:8058;
(h) Yan X, Liu G, Hu J, Willson CG. Macromolecules 2006;39:1906.
[19] Hameed N, Guo Q. Polymer 2008;49:922.
[20] Lefèvre N, Fustin CA, Varshney SK, Gohy JF. Polymer 2007;48:2306.
[21] Yao X, Chen D, Jiang M. Macromolecules 2004;37:4211.
[22] (a) Gao L, Shi L, Zhang W, An Y, Jiang X. Macromol Chem Phys 2006;207:521;
(b) Torrens F, Abad C, Codoner A, Lopera RG, Campos A. Eur Polym J 2005;41:439;
(c) Zhang L, Eisenberg A. Macromolecules 1996;29:8805;
(d) Zhang L, Shen H, Eisenberg A. Macromolecules 1997;30:1001.
[23] (a) Voets IK, van der Burgh S, Farago B, Fokkink R, Kovacevic D, Hellweg T, et al. Macromolecules 2007;40:8476;
(b) Voets IK, de Keizer A, de Waard P, Frederik PM, Bomans PHH, Schmalz H, et al. Angew Chem Int Ed 2006;45:6673.
[24] (a) Berne BJ, Pecora R. Dynamic light scattering. New York: Plenum Press; 1976;
(b) Koppel DE. J Chem Phys 1972;57:4814.
[25] Lee JY, Painter PC, Coleman MM. Macromolecules 1988;21:954.
[26] Cesteros LC, Meaurio E, Katime I. Macromolecules 1993;26:2323.
[27] (a) Kuo SW, Huang CF, Chang FC. J Polym Sci Part B Polym Phys 2001;39:1348;
(b) Kuo SW, Huang CF, Lu CH, Lin HM, Jeong KU, Chang FC. Macromol Chem Phys 2006;207:2006;
(c) He Y, Zhu B, Inoue Y. Prog Polym Sci 2004;29:1021.